

Effects of strong magnetic field on the formation of wakes in thermal QCD

Mujeeb Hasan¹ and Binoy Krishna Patra²

Department of Physics, Indian Institute of Technology Roorkee, Roorkee 247 667, India

Abstract

We have investigated how the wakes in the induced charge density and in the potential due to the passage of highly energetic partons through a thermal QCD medium get affected by the presence of strong magnetic field (B). For that purpose, we wish to analyze first the dielectric responses of the medium both in presence and absence of strong magnetic field. Therefore, we have revisited the general form for the gluon self-energy tensor at finite temperature and finite magnetic field and then calculate the relevant structure functions at finite temperature and strong magnetic field limit (SMF: $|q_f B| \gg T^2$ as well as $|q_f B| \gg m_f^2$, $q_f(m_f)$ is the electric charge (mass) of f -th flavour). We found that for slow moving partons, the real part of dielectric function is not affected by the magnetic field whereas for fast moving partons, for small $|\mathbf{k}|$, it becomes very large and approaches towards its counterpart at $B = 0$, for large $|\mathbf{k}|$. On the other hand the imaginary part is decreased for both slow and fast moving partons, due to the fact that the imaginary contribution due to quark-loop vanishes. With these ingredients, we found that the oscillation in the (scaled) induced charge density, due to the very fast partons becomes less pronounced in the presence of strong magnetic field whereas for smaller parton velocity, no significant change is observed. For the (scaled) wake potential along the motion of fast moving partons (which is of Lennard-Jones (LJ) type), the depth of negative minimum in the backward region gets reduced drastically, resulting in the reduction of the amplitude of oscillation. On the other hand in the forward region, it remains as the screened Coulomb one, except the screening now becomes much stronger for higher parton velocity. Similarly for the wake potential transverse to the motion of partons in both forward and backward regions, the depth of LJ potential for fast moving partons gets decreased severely, but still retains the forward-backward symmetry. However, for lower parton velocity, the magnetic field does not affect it significantly.

PACS: 12.39.-x, 11.10.St, 12.38.Mh, 12.39.Pn 12.75.N, 12.38.G

Keywords: Thermal QCD, Strong magnetic field, Gluon self-energy, Dielectric function, Induced charge density, Wake potential

¹mhasan@ph.iitr.ac.in

²binoy@ph.iitr.ac.in

1 Introduction

Ultra-relativistic heavy-ion collisions (URHICs) at RHIC, e-RHIC, LHC, upcoming FAIR etc. provides an enticing opportunity to identify the transition from the hadronic matter to the quark matter, known as quark-gluon plasma (QGP). The hard scatterings at the early stages of URHICs produce very high energetic partons, known as jets. The jets behave as an external hard probe, and while ploughing through the medium, it may lose energy and momentum either through the radiation [1–6] or the collision [7, 8] or both [9–11] depending on the range of momentum, altogether known as jet quenching [7, 12, 13] and have been manifested largely by the suppression of high p_T hadronic yields [14]. One of the specific consequences of the jet quenching is the dihadron azimuthal correlation at RHIC, which is manifested in the hadron pair-distribution in the intermediate p_T range through a double peak structure in the away side [15, 16]. Although, how the jet-medium interaction affects the distribution is not a settled issue, nevertheless the coupling of jets to a strongly interacting medium either at the particle level or at the collective level may explain the modification of the angular distribution [17–25], the formation of Mach cones [19–21], Cerenkov radiation [22, 23] etc., which can therefore be of phenomenological interest for the present experimental program at RHIC, LHC.

In addition, the jets, while traversing through the QGP, will disturb the charge distribution around it and create the spikes in the induced charge density, hence in the screening potential, known as wakes, which can reveal the properties of medium. The wakes in both induced charge and current densities were first investigated by Ruppert et al. [24] within the framework of linear response theory for a simple minded hot QCD medium for both weakly coupled and strongly coupled descriptions in the HTL calculations and in the theory for quantum liquid, respectively. In the same spirit, the wakes in the charge density and the potential was subsequently studied by Chakraborty et al. [26]. The wake potential is discussed in the literature by incorporating varieties of physical effects, *viz.* the nonabelian effects from the resummation calculation [27], the collisional effects [28], the momentum anisotropy [29, 30], the viscous effects [31], strongly-coupled nature of the medium in AdS/CFT framework [32] etc.

All the studies discussed hereinabove are suited for the fully central collisions, where the net baryon density is negligibly small and the chance for producing strong magnetic field is very bleak, due to the symmetric configurations in central collisions. In reality, a tiny fraction of events are truly central, in fact, most collisions occur with a nonzero impact parameter or centrality. When the two highly charged ions with extreme relativistic velocities collide noncentrally, an extremely large magnetic field ranging from m_π^2 ($\simeq 10^{18}$ Gauss) to $15 m_\pi^2$ are expected to be produced at RHIC and LHC, respectively, at the very early stages of the collisions [33, 34]. However, earlier works [35, 36] did not emphasize much on the effects of *strong* magnetic field especially produced in relativistic heavy-ion collisions on thermal QCD because the life-span of the strong magnetic field was too short to have any observable consequences in the heavy-ion phenomenology. They explained the short span of the strong magnetic field by the fact that the time (at the very early stages of the collisions) at which the magnetic field could be produced, the medium is yet to form, as a result the magnetic field decays in vacuum very fast. However some recent theoretical calculations predict that a thermal medium could have produced as early as the production of magnetic field so the electrical transport properties of the medium plays a vital role about the longevity of the magnetic field [36, 37]. Consequently many theoretical works have started emerging

to explore the effects of strong and long-lived magnetic field on QCD phenomena [38–41], which could be verified experimentally in relativistic heavy ion collisions at RHIC and LHC. Thus we get motivated to explore the effect of strong magnetic field on the abovementioned studies of wakes in charge density and potential because the jets are also produced at the time when magnetic field is produced. For that purpose we have first analyzed the response of the medium due to the passage of moving partons through the medium in the presence of strong magnetic field by the dielectric function, whose evaluation is made complete by the estimation of the gluon self-energy in the similar environment. Once the tools are ready, we explore the effects of strong magnetic field on the wakes. The first noticeable observation is that the oscillation in the (scaled) induced charge density due to the faster partons becomes less pronounced in the presence of strong magnetic field whereas for smaller parton velocity, the effect is minimal. The second observation in the (scaled) wake potential for very fast moving partons along the parallel direction in the backward region is that the large depth of negative minimum of the Lennard-Jones (LJ) potential is reduced drastically, leaving the forward region almost unaffected, except that the screening now becomes stronger. The third observation for the same in the perpendicular direction is that in both forward and backward regions, the depth of LJ type potential gets decreased severely, but still retains the forward-backward symmetry, as in the case for no magnetic field. In brief, the wakes in the induced charge density and in the potential as well have been changed significantly in the presence of strong magnetic field. Therefore this observation may serve as a signal of the existence of strong magnetic field by the revisit of the correlations between high p_T secondary particles in the pseudorapidity and azimuthal plane.

Our work proceeds as follows: First we have discussed the dielectric response due to the passage of the moving partons in a thermal QCD in an ambience of strong and homogeneous magnetic field in Section 2, wherein we have revisited the form of the gluon self-energy tensor at finite temperature (T) and finite magnetic field (B), and then calculate both real and imaginary parts of its longitudinal component at finite T and strong B in subsection 2.1. Hence the real and imaginary parts of complex dielectric function have been computed in subsection 2.2, which in turn facilitate to see the effects of strong magnetic field on the induced charged density and the resulting wake potential in the coordinate space, in subsections 3.1 and 3.2, respectively. Finally we conclude in Section 4.

2 Dielectric response of thermal QCD in an ambience of strong and homogeneous magnetic field

If the external disturbance is very small then the dielectric response of the medium can be envisaged by the dielectric tensor, ϵ^{ij} , whose longitudinal and transverse components can be extracted by the linear response theory [42–44]

$$\epsilon^{\text{Longitudinal}}(k_0, \mathbf{k}) = 1 - \frac{\Pi^{\text{Longitudinal}}(k_0, \mathbf{k})}{\mathbf{k}^2}, \quad (1)$$

$$\epsilon^{\text{Transverse}}(k_0, \mathbf{k}) = 1 - \frac{\Pi^{\text{Transverse}}(k_0, \mathbf{k})}{k_0^2}, \quad (2)$$

where the respective self-energies, $\Pi^{\text{Longitudinal}}$ and $\Pi^{\text{Transverse}}$ of the medium are obtained by the self energy tensor, $\Pi^{\mu\nu}$. However, we are interested in the former equation because the longitudinal equation is related to the density fluctuations in the medium, namely the space-charge field, which is our aim. Thus, we need to construct the gluon self-energy tensor in finite T and strong B , which will then give the longitudinal component.

2.1 Gluon self-energy tensor in finite T and strong B

We will revisit here how to construct the general form of the gluon self-energy tensor ($\Pi^{\mu\nu}$) for an isotropic QCD medium at finite T and finite B . For that, we first consider the absence of magnetic field and turn on the temperature through a heat bath to the vacuum. Since the heat bath generically defines a local rest frame, u^μ , so the Lorentz invariance is broken. Therefore, compared to vacuum, a larger tensor basis is needed, which is conveniently constructed by the available four-vectors, k^μ , u^μ and the tensor, $g^{\mu\nu}$ by the two orthogonal tensors, compatible with the physical degree of freedom, *namely* [45, 46]

$$P_L^{\mu\nu}(k) = -\frac{k^0}{\mathbf{k}^2}(k^\mu u^\nu + u^\mu k^\nu) + \frac{1}{\mathbf{k}^2} \left[\frac{(k^0)^2}{k^2} k^\mu k^\nu + k^2 u^\mu u^\nu \right], \quad (3)$$

$$P_T^{\mu\nu}(k) = -g^{\mu\nu} + \frac{k^0}{\mathbf{k}^2}(k^\mu u^\nu + u^\mu k^\nu) - \frac{1}{\mathbf{k}^2}(k^\mu k^\nu + k^2 u^\mu u^\nu), \quad (4)$$

such a way that they satisfy the 4-dimensional transversality condition - $k_\mu P_{T,L}^{\mu\nu} = 0$. The superscripts T and L represent the transverse and longitudinal with respect to the three-momentum (\mathbf{k}), respectively. Thus the self-energy tensor at finite temperature is written in the above basis

$$\Pi^{\mu\nu}(k_0, \mathbf{k}) = P_T^{\mu\nu} \Pi^T(k_0, \mathbf{k}) + P_L^{\mu\nu} \Pi^L(k_0, \mathbf{k}), \quad (5)$$

where the structure factors, Π^T and Π^L are obtained by evaluating the quark-loop, gluon-loops with 2-gluon and 3-gluon vertices and ghost-loop contributions in HTL approximation with the temperature as the hard scale for the loop momenta³ for both gluons and quarks.

Now the presence of the magnetic field breaks the rotational symmetry in the system because it introduces an anisotropy in space. Thus, one can define a new four vector b^μ which is associated with the electromagnetic field tensor $F^{\mu\nu}$. In the rest frame of the heat bath, i.e., $u^\mu = (1, 0, 0, 0)$, b^μ can be defined uniquely as projection of $\tilde{F}_{\mu\nu}$ along u^ν ,

$$b_\mu = \frac{1}{2B} \epsilon_{\mu\nu\rho\lambda} u^\nu F^{\rho\lambda} = \frac{1}{B} u^\nu \tilde{F}_{\mu\nu} = (0, 0, 0, 1).$$

Hence, much larger basis is needed and can be constructed with the vectors, k^μ , u^μ , b^μ and the tensor, $g^{\mu\nu}$. Therefore, in addition to $P_T^{\mu\nu}$ and $P_L^{\mu\nu}$ at finite temperature, two more tensors, $P_{\parallel}^{\mu\nu}$

³In pure thermal medium, the gluon loop-momenta may be hard, $\mathcal{O}(T)$ or soft, $\mathcal{O}(g'T)$ because the Matsubara frequencies ($2m\pi T$) are integral multiples of $2\pi T$. Thus, the hard (soft)-momentum regime requires $m \neq 0$ ($m = 0$) bosonic matsubara mode. On the other hand the quark loop-momenta will always be hard, even for $m = 0$ Matsubara fermionic mode.

and $P_{\perp}^{\mu\nu}$ are recently constructed in [47, 48] for the leading-order perturbation theory

$$\begin{aligned} P_{\parallel}^{\mu\nu}(k) &= -\frac{k^0 k^z}{k_{\parallel}^2} (b^{\mu} u^{\nu} + u^{\mu} b^{\nu}) + \frac{1}{k_{\parallel}^2} [(k^0)^2 b^{\mu} b^{\nu} + (k^z)^2 u^{\mu} u^{\nu}], \\ &= -\left(g_{\parallel}^{\mu\nu} - \frac{k_{\parallel}^{\mu} k_{\parallel}^{\nu}}{k_{\parallel}^2} \right), \end{aligned} \quad (6)$$

$$\begin{aligned} P_{\perp}^{\mu\nu}(k) &= \frac{1}{k_{\perp}^2} [-k_{\perp}^2 g^{\mu\nu} + k^0 (k^{\mu} u^{\nu} + u^{\mu} k^{\nu}) - k^z (k^{\mu} b^{\nu} + b^{\mu} k^{\nu}) + k^0 k^z (b^{\mu} u^{\nu} + u^{\mu} b^{\nu}) \\ &\quad - k^{\mu} k^{\nu} + (k_{\perp}^2 - (k^0)^2) u^{\mu} u^{\nu} - \mathbf{k}^2 b^{\mu} b^{\nu}], \\ &= -\left(g_{\perp}^{\mu\nu} - \frac{k_{\perp}^{\mu} k_{\perp}^{\nu}}{k_{\perp}^2} \right), \end{aligned} \quad (7)$$

by demanding the same transversality condition for all tensors. The notations used in the above equations are as follows:

$$g_{\parallel}^{\mu\nu} = \text{diag}(1, 0, 0, -1), \quad g_{\perp}^{\mu\nu} = \text{diag}(0, -1, -1, 0), \quad k_{\parallel}^2 = (k_0)^2 - (k_z)^2, \quad k_{\perp}^2 = (k_x)^2 + (k_y)^2.$$

Unlike the thermal medium in the absence of magnetic field, where both quark and gluon degrees of freedom have been treated in equal footing in hard thermal loop approximation, quark and gluon degrees of freedom are treated differently in presence of magnetic field because only quarks get affected by the magnetic field and gluons remain unaffected. Thus in the presence of strong magnetic field, the hard scale for the quark-loop momentum will be provided by the magnetic field whereas the hard scale for the gluon-loop momentum is still given by the temperature. As a result the quark and gluon loops (denoted by q and g , respectively) get separated in the general form of gluon self-energy tensor in finite T and strong B

$$\Pi^{\mu\nu}(k) = P_L^{\mu\nu} \Pi^{g,L}(k) + P_T^{\mu\nu} \Pi^{g,T}(k) + P_{\parallel}^{\mu\nu} \Pi^{q,\parallel}(k) + P_{\perp}^{\mu\nu} \Pi^{q,\perp}(k), \quad (8)$$

where the two new structure factors, $\Pi^{q,\parallel}$ and $\Pi^{q,\perp}$ give the contributions in the gluon self-energy due to the magnetic field only and their evaluation will be made from the quark loop and the thermal contribution is still given by $\Pi^{g,L}$ and $\Pi^{g,T}$, whose evaluations are done by the gluon (and ghost) loop only.

In the strong magnetic field, the quarks are constrained to be in the lowest Landau level (LLL) ($n = 0$) only, which is witnessed by the vanishing of the momentum transverse to the magnetic field ($p_{\perp} = 0$) in the dispersion relation ($E_0 = \sqrt{p_z^2 + m_f^2}$). This causes the structure factor, $\Pi^{q,\perp}$ vanishingly small ($\Pi^{q,\perp} \approx 0$), therefore, the longitudinal component ($\mu = \nu = 0$, denoted by L') of the gluon self-energy tensor at finite T and strong magnetic field (B) in equation (8) is written in terms of nonvanishing quark (q) and gluon (g) loops contributions

$$\Pi^{L'}(k) = \Pi^{q,\parallel}(k) + \Pi^{g,L}(k), \quad (9)$$

because $P_T^{00}, P_{\perp}^{00} = 0$.

We will now calculate the longitudinal component (denoted by \parallel) of the quark-loop contribution in the self-energy - $\Pi^{q,\parallel}$ in the real-time formalism. So we start with the “11”-component of the

quark-propagator matrix in thermal QCD in presence of strong magnetic field,

$$iS_{11}(p) = \left[\frac{1}{p_{\parallel}^2 - m_f^2 + i\epsilon} + 2\pi i n(p_0) \delta(p_{\parallel}^2 - m_f^2) \right] (1 + \gamma^0 \gamma^3 \gamma^5) (\gamma^0 p_0 - \gamma^3 p_z + m_f) e^{\frac{-p_{\perp}^2}{|q_f B|}}. \quad (10)$$

Hence the “11”-component of the self-energy matrix due to the quark-loop will be (omitting the label “11”)

$$\begin{aligned} \Pi^{q,\mu\nu}(k) &= \frac{ig^2}{2} \sum_f \int \frac{d^4 p}{(2\pi)^4} \text{Tr}[\gamma^\mu S_{11}(p) \gamma^\nu S_{11}(q)] \\ &= \frac{ig^2}{2} \sum_f \int \frac{d^4 p}{(2\pi)^4} \text{Tr}[(\gamma^\mu (1 + \gamma^0 \gamma^3 \gamma^5) (\gamma^0 p_0 - \gamma^3 p_z + m_f) \gamma^\nu (1 + \gamma^0 \gamma^3 \gamma^5) (\gamma^0 q_0 - \gamma^3 q_z + m_f)] \\ &\quad \left\{ \frac{1}{p_{\parallel}^2 - m_f^2 + i\epsilon} + 2\pi i n(p_0) \delta(p_{\parallel}^2 - m_f^2) \right\} \left\{ \frac{1}{q_{\parallel}^2 - m_f^2 + i\epsilon} + 2\pi i n(q_0) \delta(q_{\parallel}^2 - m_f^2) \right\} e^{\frac{-p_{\perp}^2 - q_{\perp}^2}{|q_f B|}} \end{aligned} \quad (11)$$

where the trace over the γ matrices is calculated as

$$L^{\mu\nu} = 8 \left[p_{\parallel}^{\mu} q_{\parallel}^{\nu} + p_{\parallel}^{\nu} q_{\parallel}^{\mu} - g_{\parallel}^{\mu\nu} ((p \cdot q)_{\parallel} - m_f^2) \right]. \quad (12)$$

It is to be noted here that the coupling (g) in equation (11) depends on the magnetic field only because as mentioned above the dominant scale for quarks in strong magnetic limit ($|q_f B| \gg T^2$) is the scale related to magnetic field ($|q_f B|$). Moreover the coupling, g depends only on the momentum longitudinal to the magnetic field ⁴ in the following manner [50]

$$\alpha_s^{\parallel}(eB) = \frac{g^2}{4\pi} = \frac{1}{\alpha_s^0(\mu_0)^{-1} + \frac{11N_c}{12\pi} \ln\left(\frac{k_z^2 + M_B^2}{\mu_0^2}\right) + \frac{1}{3\pi} \sum_f \frac{|q_f B|}{\sigma}}, \quad (13)$$

where

$$\alpha_s^0(\mu_0) = \frac{12\pi}{11N_c \ln\left(\frac{(\mu_0^2 + M_B^2)}{\Lambda_V^2}\right)}. \quad (14)$$

where $k_z = 0.1\sqrt{eB}$, $\mu_0 = 1.1$ GeV, $\Lambda_V = 0.385$ GeV, $M_B \sim 1$ GeV and the string tension, $\sigma = 0.18\text{GeV}^2$.

Due to the presence of magnetic field, the quark-loop momentum (p) becomes factorizable into parallel and perpendicular with respect to the magnetic field. As a result, the tensor, $\Pi^{q,\mu\nu}(k)$ in (11) also becomes factorizable, *namely*

$$\Pi^{q,\mu\nu}(k) = \sum_f \Pi^{q,\mu\nu}(k_{\parallel}) A(k_{\perp}), \quad (15)$$

where the perpendicular component of loop momentum (p_{\perp}) is integrated out to give rise the factor, $A(k_{\perp})$

$$A(k_{\perp}) = \frac{\pi |q_f B|}{2} e^{-\frac{k_{\perp}^2}{2|q_f B|}}, \quad (16)$$

⁴because in strong magnetic field limit, only the lowest Landau level (LLL) is occupied and hence the dispersion relation manifests the vanishing of the transverse component of momentum.

which, in SMF approximation ($\exp(-\frac{k_\perp^2}{2|q_f|B}) \approx 1$), becomes

$$A(k_\perp) = \frac{\pi|q_f|B}{2}. \quad (17)$$

The part of the self energy that depends only on the parallel component of momentum, $\Pi^{q,\mu\nu}(k_\parallel)$ due to quark-loop is decomposed into vacuum and medium components, *say*

$$\Pi^{q,\mu\nu}(k_\parallel) \equiv \Pi_V^{q,\mu\nu}(k_\parallel) + \Pi_n^{q,\mu\nu}(k_\parallel) + \Pi_{n^2}^{q,\mu\nu}(k_\parallel), \quad (18)$$

where the vacuum and thermal contributions due to single and double distribution functions, respectively, are

$$\Pi_V^{q,\mu\nu}(k_\parallel) = \frac{ig^2}{2(2\pi)^4} \int dp_0 dp_z L^{\mu\nu} \left\{ \frac{1}{(q_\parallel^2 - m_f^2 + i\epsilon)} \frac{1}{(p_\parallel^2 - m_f^2 + i\epsilon)} \right\}, \quad (19)$$

$$\Pi_n^{q,\mu\nu}(k_\parallel) = \frac{ig^2(2\pi i)}{2(2\pi)^4} \int dp_0 dp_z L^{\mu\nu} \left\{ n(p_0) \frac{\delta(p_\parallel^2 - m_f^2)}{(q_\parallel^2 - m_f^2 + i\epsilon)} + n(q_0) \frac{\delta(q_\parallel^2 - m_f^2)}{(p_\parallel^2 - m_f^2 + i\epsilon)} \right\}, \quad (20)$$

$$\Pi_{n^2}^{q,\mu\nu}(k_\parallel) = \frac{ig^2}{2(2\pi)^4} \int dp_0 dp_z L^{\mu\nu} \{ (-4\pi^2) n(p_0) n(q_0) \delta(p_\parallel^2 - m_f^2) \delta(q_\parallel^2 - m_f^2) \}. \quad (21)$$

Now we obtain the-real part of the vacuum term (19) as

$$\Re \Pi_V^{q,\mu\nu}(k_\parallel) = \left(g_\parallel^{\mu\nu} - \frac{k_\parallel^\mu k_\parallel^\nu}{k_\parallel^2} \right) \frac{g^2}{2\pi^3} \left[\frac{2m_f^2}{k_\parallel^2} \left(1 - \frac{4m_f^2}{k_\parallel^2} \right)^{-\frac{1}{2}} \left\{ \ln \frac{\left(1 - \frac{4m_f^2}{k_\parallel^2} \right)^{1/2} - 1}{\left(1 - \frac{4m_f^2}{k_\parallel^2} \right)^{1/2} + 1} \right\} + 1 \right], \quad (22)$$

which was also calculated in [48, 51–54]. Thus after multiplying the transverse momentum factor (17), the longitudinal component of the real-part of the vacuum term for massless quarks ($m_f = 0$) is obtained in the simplified form

$$\Re \Pi_V^{q,\parallel}(k_0, k_z) = \frac{g^2}{4\pi^2} \sum_f |q_f B| \frac{k_z^2}{k_\parallel^2}, \quad (23)$$

whereas the imaginary-part vanishes

$$\Im \Pi_V^{q,\parallel}(k_0, k_z) = 0. \quad (24)$$

Now we will calculate the medium contribution due to single distribution function, so we start with the real-part of the longitudinal component from (20) as

$$\begin{aligned} \Re \Pi_n^{q,\parallel}(k_\parallel) &= -\frac{g^2}{2(2\pi)^3} \int dp_0 dp_z L^{00} \left[n(p_0) \frac{\left\{ \delta(p_0 - \omega_p) + \delta(p_0 + \omega_p) \right\}}{2\omega_p(q_0^2 - q_z^2 - m_f^2)} \right. \\ &\quad \left. + n(q_0) \frac{\left\{ \delta(q_0 - \omega_q) + \delta(q_0 + \omega_q) \right\}}{2\omega_q(p_0^2 - p_z^2 - m_f^2)} \right], \end{aligned} \quad (25)$$

with the following notations:

$$\begin{aligned} L^{00} &= 8[p_0 q_0 + p_z q_z + m_f^2], \\ \omega_p &= \sqrt{p_z^2 + m_f^2}, \\ \omega_q &= \sqrt{q_z^2 + m_f^2} = \sqrt{(p_z - k_z)^2 + m_f^2}. \end{aligned}$$

After performing the p_0 integration first, the above Eq.(25) becomes a one-dimensional equation in p_z

$$\begin{aligned} \Re\Pi_n^{q,\parallel}(k_{\parallel}) &= -\frac{g^2}{2(2\pi)^3} \int dp_z \left[\frac{L^{00}(p_0 = \omega_p) n(p_0 = \omega_p)}{2\omega_p[(\omega_p - k_0)^2 - \omega_q^2]} + \frac{L^{00}(p_0 = -\omega_p) n(p_0 = -\omega_p)}{2\omega_p[(\omega_p + k_0)^2 - \omega_q^2]} \right. \\ &\quad \left. + \frac{L^{00}(p_0 = \omega_q + k_0) n(q_0 = \omega_q)}{2\omega_q[(\omega_q + k_0)^2 - \omega_p^2]} + \frac{L^{00}(p_0 = -\omega_q + k_0) n(q_0 = -\omega_q)}{2\omega_q[(\omega_q - k_0)^2 - \omega_p^2]} \right]. \end{aligned} \quad (26)$$

We will now evaluate the p_z integration in the massless limit ($m_f = 0$). So, the following quantities are calculated for $m_f = 0$ as

$$\begin{aligned} L^{00}(p_0 = p_z) &= 8[2p_z^2 - p_z k_0 - p_z k_z], \\ L^{00}(p_0 = p_z) &= 8[2p_z^2 + p_z k_0 - p_z k_z], \\ L^{00}(p_0 = q_z + k_0) &= 8[2p_z^2 + k_z^2 - 3p_z k_z + q_z k_0], \\ L^{00}(p_0 = -q_z + k_0) &= 8[2p_z^2 + k_z^2 - 3p_z k_z - q_z k_0], \end{aligned}$$

and then substituting them in Eq.(26), the medium term becomes in the massless limit

$$\begin{aligned} \Re\Pi_n^{q,\parallel}(k_{\parallel}) &= -\frac{4g^2}{2(2\pi)^3} \int dp_z \left[\frac{(2p_z - k_0 - k_z) n(p_0 = p_z)}{[(p_z - k_0)^2 - (p_z - k_z)^2]} + \frac{(2p_z + k_0 - k_z) n(p_0 = -p_z)}{[(p_z + k_0)^2 - (p_z - k_z)^2]} \right. \\ &\quad \left. + \frac{(2p_z^2 + k_z^2 - 3p_z k_z + q_z k_0) n(q_0 = q_z)}{[(q_z + k_0)^2 - p_z^2] q_z} + \frac{(2p_z^2 + k_z^2 - 3p_z k_z - q_z k_0) n(q_0 = -q_z)}{[(q_z - k_0)^2 - p_z^2] q_z} \right] \end{aligned} \quad (27)$$

After further simplification, the above equation yields into a nicer form

$$\Re\Pi_n^{q,\parallel}(k_{\parallel}) = -\frac{2g^2}{(2\pi)^3} \int dp_z \left[-\frac{n(p_0 = p_z)}{(k_0 - k_z)} + \frac{n(p_0 = -p_z)}{(k_0 + k_z)} + \frac{n(q_0 = q_z)}{(k_0 - k_z)} - \frac{n(q_0 = -q_z)}{(k_0 + k_z)} \right]. \quad (28)$$

After substituting the distribution function, the medium contribution for the quark-loop is found to vanish identically

$$\begin{aligned} \Re\Pi_n^{q,\parallel}(k_{\parallel}) &= -\frac{4g^2}{(2\pi)^3} \frac{k_z T}{k_0^2 - k_z^2} \left(\int_{-\infty}^{\infty} dt \frac{1}{e^t + 1} - \int_{-\infty}^{\infty} dt' \frac{1}{e^{t'} + 1} \right), \\ &= 0. \end{aligned} \quad (29)$$

This result thus demonstrates the results of (1+1) dimensional massless QED (also known as Schwinger model), where the medium does not permeate to the vacuum. The same thing happens

herein above because the (3+1) dimensional QCD (in quark-loop) in strong magnetic field gets reduced into a (1+1) dimensional (longitudinal) QCD, *mimicking* the Schwinger model.

On the other hand, the imaginary part due to single distribution function (20) also vanishes

$$\Im \Pi_n^{q,\parallel}(k_0, k_z) = 0. \quad (30)$$

The medium contribution involving the product of two distribution functions (21) does not contribute to the real-part of the self-energy, i.e.

$$\Re \Pi_{n^2}^{q,\parallel}(k_0, k_z) = 0, \quad (31)$$

whereas the computation of the imaginary-part is effective boiled down to the problem of one-loop massless fermion loop in two dimension as an artifact of strong magnetic field. Hence the mapping of two-dimensional massless fermion into bosons, known as CJT formalism of bosonization [55] helps to calculate the above imaginary-part. The bosonization technique was earlier well documented in [56, 57]. Very recently this technique is applied to QCD in a strong magnetic field [58], where the imaginary-part is obtained from the retarded current-current correlator as

$$\Im \Pi_{n^2}^{q,\parallel}(k_0, k_z) = -\frac{g^2 \sum_f |q_f| B}{8\pi} k_0 [\delta(k_0 - k_z) + \delta(k_0 + k_z)], \quad (32)$$

where the factor $|q_f B|/8\pi$ is the transverse density of states for the LLL states and arises due to the decoupling of the transverse dynamics from the longitudinal dynamics of LLL states.

We have thus finally obtained the real-part of the quark-loop contribution by the vacuum (23) contribution only, *i.e.*

$$\begin{aligned} \Re \Pi^{q,\parallel}(k_0, k_z) &= \Re \Pi_V^{q,\parallel}(k_0, k_z), \\ &= \frac{g^2}{4\pi^2} \sum_f |q_f| B \frac{k_z^2}{k_{\parallel}^2}, \end{aligned} \quad (33)$$

and the imaginary-part of the quark-loop contribution is given by the n^2 contribution

$$\begin{aligned} \Im \Pi^{q,\parallel}(k_0, k_z) &= \Im \Pi_{n^2}^{q,\parallel}(k_0, k_z), \\ &= \frac{-g^2 \sum_f |q_f| B}{8\pi} k_0 [\delta(k_0 - k_z) + \delta(k_0 + k_z)]. \end{aligned} \quad (34)$$

The above real and imaginary parts have also been addressed earlier in [59]. Both of these real- and imaginary-parts of quark-loop contribution are indeed devoid of medium (temperature) correction which out to be for the dynamics of massless quarks in (1+1) dimension.

Now let us calculate the remaining contribution by the gluon-loop, $\Pi^{g,L}$ in (9). Since the gluons are unaffected by the magnetic field so we calculate from the HTL perturbation theory, which is calculated earlier in [60–62], and is given by

$$\Pi^{g,L}(k_0, \mathbf{k}) = g'^2 T^2 \left(\frac{k_0}{2|\mathbf{k}|} \ln \frac{k_0 + |\mathbf{k}| + i\epsilon}{k_0 - |\mathbf{k}| + i\epsilon} - 1 \right), \quad (35)$$

whose real- and imaginary-parts can be extracted by the identity:

$$\ln \left(\frac{k_0 + |\mathbf{k}| \pm i\epsilon}{k_0 - |\mathbf{k}| \pm i\epsilon} \right) = \ln \left| \frac{k_0 + |\mathbf{k}|}{k_0 - |\mathbf{k}|} \right| \mp i\pi\theta(\mathbf{k}^2 - k_0^2), \quad (36)$$

Thus the real- and imaginary-parts are obtained from (35) as

$$\Re \Pi^{g,L}(k_0, \mathbf{k}) = g'^2 T^2 \left(\frac{k_0}{2|\mathbf{k}|} \ln \left| \frac{k_0 + |\mathbf{k}|}{k_0 - |\mathbf{k}|} \right| - 1 \right), \quad (37)$$

$$\Im \Pi^{g,L}(k_0, \mathbf{k}) = -g'^2 T^2 \frac{\pi k_0}{2|\mathbf{k}|}, \quad (38)$$

where the strong coupling, g' runs only with the temperature (*unlike* g), and its one-loop expression is given by [63]

$$\alpha'(T) = \frac{g'^2(T)}{4\pi} = \frac{6\pi}{(33 - 2N_f) \ln(\frac{2\pi T}{\Lambda_{QCD}})}, \quad (39)$$

with N_f is the number of flavour and $\Lambda_{QCD} \sim 0.200 GeV$.

Thus the real- and imaginary-part of the longitudinal component of the gluon self-energy tensor in finite T in the presence of strong B is obtained by adding the finite T correction given by (37) and (38) and strong B correction given by (33) and (34)

$$\begin{aligned} \Re \Pi^{L'}(k_0, \mathbf{k}) &= \Re \Pi^{g,L}(k_0, \mathbf{k}) + \Re \Pi^{q,\parallel}(k_0, k_z), \\ &= g'^2 T^2 \left(\frac{k_0}{2|\mathbf{k}|} \ln \left| \frac{k_0 + |\mathbf{k}|}{k_0 - |\mathbf{k}|} \right| - 1 \right) + \frac{g^2}{4\pi^2} \sum_f |q_f| B \frac{k_z^2}{k_{\parallel}^2}, \end{aligned} \quad (40)$$

$$\begin{aligned} \Im \Pi^{L'}(k_0, \mathbf{k}) &= \Im \Pi^{g,L}(k_0, \mathbf{k}) + \Im \Pi^{q,\parallel}(k_0, k_z), \\ &= -g'^2 T^2 \frac{\pi k_0}{2|\mathbf{k}|} - \frac{g^2 \sum_f |q_f| B}{8\pi} k_0 [\delta(k_0 - k_z) + \delta(k_0 + k_z)], \end{aligned} \quad (41)$$

respectively.

To decipher the effects of strong magnetic field alone, we need to know the abovementioned results of quark- and gluon-loops in the *absence* of magnetic field. The gluon-loop contribution is already mentioned above, and the quark-loop contribution can also be obtained from the gluon-loop expression in relativistic approximation, by replacing the color factor by the flavour factor. For the sake of complete comparison, the real- and imaginary-part of quark-loop contribution are

$$\Re \Pi^{q,L}(k_0, \mathbf{k}) = g'^2 T^2 \left(\frac{N_f}{6} \right) \left(\frac{k_0}{2|\mathbf{k}|} \ln \left| \frac{k_0 + |\mathbf{k}|}{k_0 - |\mathbf{k}|} \right| - 1 \right), \quad (42)$$

$$\Im \Pi^{q,L}(k_0, \mathbf{k}) = -g'^2 T^2 \left(\frac{N_f}{6} \right) \frac{\pi k_0}{2|\mathbf{k}|}. \quad (43)$$

Thus the real- and imaginary-part of the longitudinal component of the gluon self-energy tensor in finite T in the absence of B is given by adding the gluon loop contribution given by (37) and

(38) and quark loop contribution given by (42) and (43) in absence of magnetic field

$$\Re \Pi^L(k_0, \mathbf{k}) = g'^2 T^2 \left(1 + \frac{N_f}{6} \right) \left(\frac{k_0}{2|\mathbf{k}|} \ln \left| \frac{k_0 + |\mathbf{k}|}{k_0 - |\mathbf{k}|} \right| - 1 \right), \quad (44)$$

$$\Im \Pi^L(k_0, \mathbf{k}) = -g'^2 T^2 \left(1 + \frac{N_f}{6} \right) \frac{\pi k_0}{2|\mathbf{k}|}, \quad (45)$$

respectively.

Therefore, the real- and imaginary-part of the longitudinal component of gluon self-energy in the presence and absence of magnetic field thus obtained, facilitate to study analytically the dielectric response of a hot QCD medium in respective scenarios.

2.2 Dielectric response function in presence of strong magnetic field

The definition (1) give the longitudinal component of the dielectric response function, which becomes complex. The real (40) and imaginary parts (41) of the longitudinal component of the gluon self-energy tensor give the real and imaginary parts of longitudinal dielectric function in presence of strong magnetic field

$$\Re \epsilon_{B \neq 0}^{L'}(k_0, \mathbf{k}) = 1 + \frac{g'^2 T^2}{\mathbf{k}^2} \left(1 - \frac{k_0}{2|\mathbf{k}|} \ln \left| \frac{k_0 + |\mathbf{k}|}{k_0 - |\mathbf{k}|} \right| \right) - \frac{g^2}{4\pi^2} \sum_f |q_f| B \frac{1}{\mathbf{k}^2} \frac{k_z^2}{k_{\parallel}^2}, \quad (46)$$

$$\Im \epsilon_{B \neq 0}^{L'}(k_0, \mathbf{k}) = \frac{g'^2 T^2}{\mathbf{k}^2} \frac{\pi k_0}{2|\mathbf{k}|} + \frac{g^2 \sum_f |q_f| B}{8\pi} \frac{k_0}{\mathbf{k}^2} [\delta(k_0 - k_z) + \delta(k_0 + k_z)]. \quad (47)$$

Before moving on to the calculations of the induced charge density and the wake potential in the upcoming section, it is worth to mention here that due to the constraint - $k_0 = \mathbf{k} \cdot \mathbf{v}$ in the Dirac delta function, that will appear in the charge density (53) and for the choice $k_z = \mathbf{k} \cos \theta$, the quark-loop contribution in the second term of equation (47) is only nonvanishing for $v = 1$ ($v = |\mathbf{v}|$). In our work, since we have considered the parton velocities less than one ($v = 0.55, 0.99$) so the imaginary part for quark-loop contribution will give the vanishing contribution.

To see the effects of strong magnetic field alone, the real and imaginary parts of the same in the absence of magnetic field needs to be mentioned here as a baseline for comparison. These are obtained from the HTL techniques [60–62]

$$\Re \epsilon_{B=0}^L(k_0, \mathbf{k}) = 1 + \frac{g'^2 T^2}{\mathbf{k}^2} \left(1 + \frac{N_f}{6} \right) \left(1 - \frac{k_0}{2|\mathbf{k}|} \ln \left| \frac{k_0 + |\mathbf{k}|}{k_0 - |\mathbf{k}|} \right| \right), \quad (48)$$

$$\Im \epsilon_{B=0}^L(k_0, \mathbf{k}) = \frac{g'^2 T^2}{\mathbf{k}^2} \left(1 + \frac{N_f}{6} \right) \frac{\pi k_0}{2|\mathbf{k}|}. \quad (49)$$

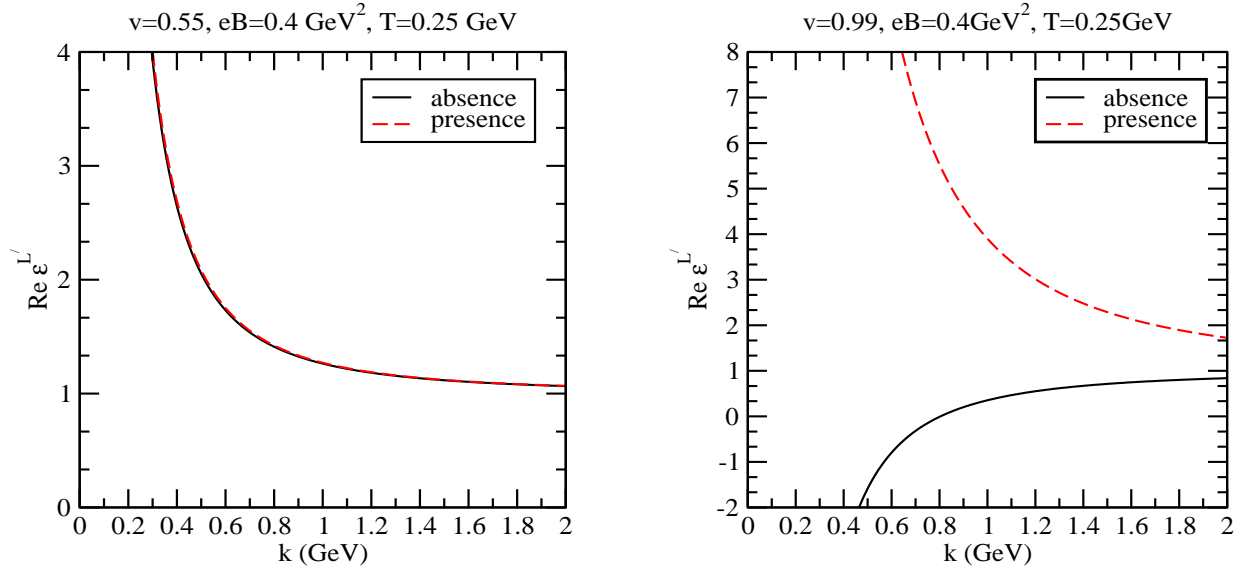


Figure 1: Real part of dielectric response function in absence and presence of strong magnetic field for $v = 0.55$ (left panel) and $v = 0.99$ (right panel), respectively.

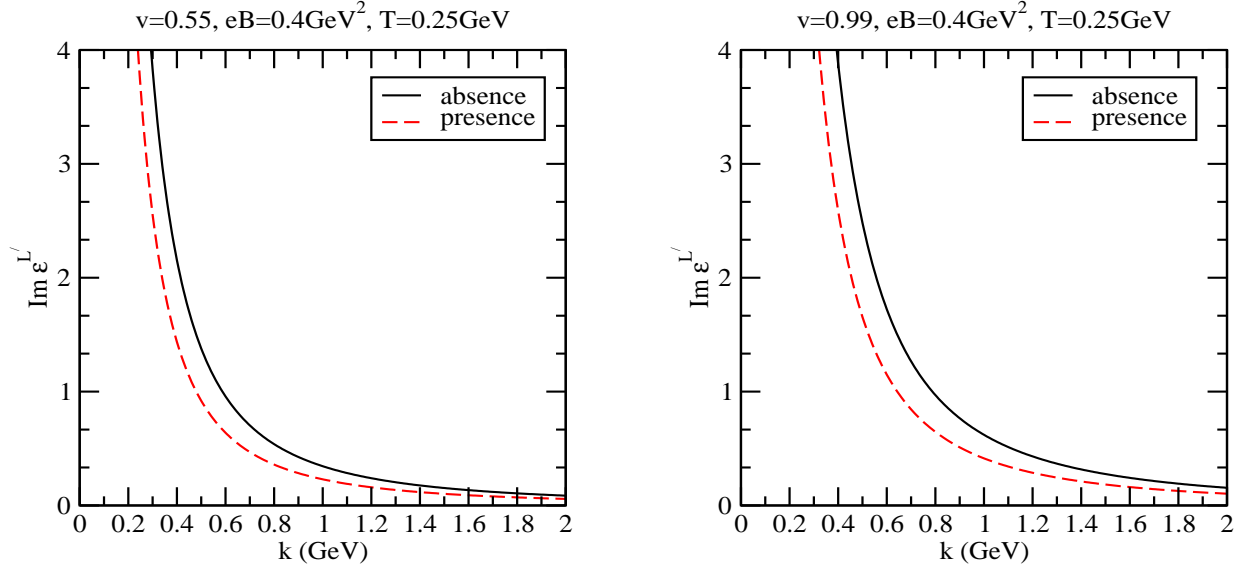


Figure 2: Imaginary part of dielectric response function in absence and presence of strong magnetic field for $v = 0.55$ (left panel) and $v = 0.99$ (right panel), respectively.

In order to see the qualitative variations of real and imaginary parts of dielectric function obtained in Eqs.(46)-(49), with the parton velocity v , we have used the constraint put by the Dirac delta function defined in Eq.(53) and $k_z = \mathbf{k} \cos \theta$. In addition to this, we have taken the vectors \mathbf{v} and \mathbf{k} along the same direction means, $\cos \theta = \chi = 1$, where the parton velocity \mathbf{v} is assumed to be in the z -direction. Thus, to see the effects of magnetic field on the dielectric function, we have computed numerically its real and imaginary parts in the absence and presence of strong magnetic for slow ($v = 0.55$) and fast ($v = 0.99$) moving partons in Fig.1 and Fig.2, respectively. For $v = 0.55$, the change in the real part is meagre as compared to the case of no magnetic field. On the other hand, for $v = 0.99$, its magnitude becomes much larger and the variation also becomes opposite compared to its counterpart in the absence of magnetic field. The above anomalous behaviour of the real part of dielectric function can be understood physically in the following way: In the absence of magnetic field both quark and gluon loops in HTL approximation have been treated on the same footing, apart from the color and flavour factors, so the momentum dependence for the real part of both loops (in equations (37) and (42)) are the same which, in terms of velocity, look like ($\chi = \cos \theta$, θ is angle between \mathbf{v} and \mathbf{k} , mentioned later in equation (53))

$$\Re \Pi^{g(q),L}(v, \chi) \sim \left(\frac{v\chi}{2} \ln \left| \frac{v\chi + 1}{v\chi - 1} \right| - 1 \right). \quad (50)$$

In presence of strong magnetic field, gluon loop is unaffected but the quark loop gets affected by the strong magnetic field (as seen in equation (33)), which in turn in terms of velocity looks as

$$\Re \Pi^{q,\parallel}(v) \sim \frac{1}{v^2 - 1}, \quad (51)$$

which can be understood by the fact that the momentum integration in quark-loop becomes one dimensional as an artifact of phase-space reduction in strong magnetic field, unlike the full three-dimensional momentum integration in the absence of strong magnetic field. As a result, the quark-loop contribution in the (real part) dielectric function becomes much larger than its counterpart in the absence of magnetic field for velocity (v) closer to c ($v = 0.99$).

More specifically, for small $|\mathbf{k}|$, the real part becomes very large and approaches towards its counterpart at $B = 0$, for large $|\mathbf{k}|$. On the other hand, the imaginary part gets decreased for both slow and fast moving partons, due to the fact that the imaginary contribution due to quark-loop vanishes. However, for larger parton velocity, its magnitude in both absence and presence of magnetic field increases. In brief, only the real part of dielectric function for higher value of parton velocity is largely affected, whose ramifications will now be explored in both induced color charge density and wake potential in next section.

3 Wakes in the presence of strong magnetic field

When a moving test charge particle is traversing through the plasma, the charge density is induced locally, as a result a wake is observed in the potential due to the induced charge density. Both of them depend on the velocity of the moving test charge as well as the distribution of background particles, which are going to be discussed in coming subsections.

3.1 Induced color charge density

Now we are going to discuss the wakes created in the induced charge density, which can be expressed in terms of the dielectric response function $\epsilon^{L'}(k_0, \mathbf{k})$ and the external color charge density as

$$\rho_{\text{ind}}^a(k_0, \mathbf{k}) = - \left\{ 1 - \frac{1}{\epsilon^{L'}(k_0, \mathbf{k})} \right\} \rho_{\text{ext}}^a(k_0, \mathbf{k}), \quad (52)$$

where the external color charge density of charge Q^a ($a = 1, 2, \dots$) with velocity \mathbf{v} is given as

$$\rho_{\text{ext}}^a(k_0, \mathbf{k}) = 2\pi Q^a \delta(k_0 - \mathbf{k} \cdot \mathbf{v}). \quad (53)$$

Combining Eq.(52) and Eq.(53) and taking the inverse Fourier transform, we obtain the induced charge density in the coordinate space

$$\rho_{\text{ind}}^a(\mathbf{r}, t) = 2\pi Q^a \int \frac{d^3k}{(2\pi)^3} \int \frac{dk_0}{2\pi} e^{i(\mathbf{k} \cdot \mathbf{r} - k_0 t)} \left\{ \frac{1}{\epsilon^{L'}(k_0, \mathbf{k})} - 1 \right\} \delta(k_0 - \mathbf{k} \cdot \mathbf{v}). \quad (54)$$

Assuming that the partons are moving along the z-direction, *i.e.* $\mathbf{v}(0, 0, v)$ and using the cylindrical coordinate system for $\mathbf{r}(s, 0, z)$, spherical polar coordinate system for $\mathbf{k}(k \cos \phi \sin \theta, k \sin \phi \sin \theta, k \cos \theta)$, we get the induced charge density in terms of the spherical Bessel function of first kind (J_0)

$$\rho_{\text{ind}}^a(\mathbf{r}, t) = \frac{Q^a}{(2\pi)^2} \int_0^\infty k^2 dk \int_{-1}^1 d\chi J_0(ks\sqrt{1-\chi^2}) e^{i\Gamma} \left\{ \frac{1}{\epsilon^{L'}(kv\chi, \mathbf{k})} - 1 \right\}, \quad (55)$$

where the notations are defined by

$$\chi = \cos \theta, \quad \Gamma = k\chi(z - vt),$$

$$J_0(x) = \frac{1}{2\pi} \int_0^{2\pi} d\theta e^{ix \cos \theta}.$$

By decomposing the dielectric function ($\epsilon^{L'}$) into the real and imaginary parts, the scaled induced charge density, $\rho_{\text{ind}}^0(\mathbf{r}, t)$ ($= \frac{\rho_{\text{ind}}^a(\mathbf{r}, t)}{(Q^a/2\pi^2)m_D}$) is recast in the following form

$$\rho_{\text{ind}}^0(\mathbf{r}, t) = \int_0^\infty k^2 dk \int_0^1 d\chi J_0(ks\sqrt{1-\chi^2}) \left[\cos \Gamma \left\{ \frac{\Re \epsilon^{L'}(kv\chi, \mathbf{k})}{\Delta} - 1 \right\} + \sin \Gamma \frac{\Im \epsilon^{L'}(kv\chi, \mathbf{k})}{\Delta} \right], \quad (56)$$

with $\Delta = [\Re \epsilon^{L'}(kv\chi, \mathbf{k})]^2 + [\Im \epsilon^{L'}(kv\chi, \mathbf{k})]^2$.

We are now going to investigate the effects of strong magnetic field on the induced charge density quantitatively through the three-dimensional plots in Fig.3 and Fig.4 for higher and smaller parton velocities, respectively.

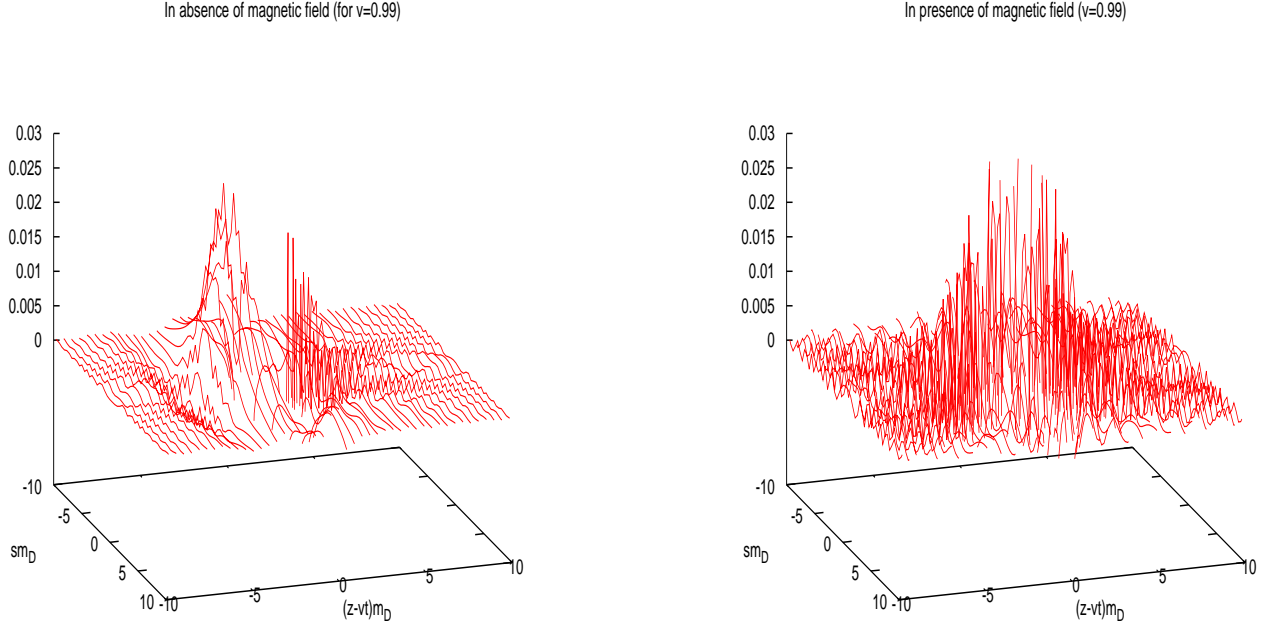


Figure 3: Scaled induced charge density (ρ_{ind}^0) in absence (Left panel) and presence (Right panel) of strong magnetic field for higher parton velocity $v = 0.99$, respectively.

For faster (than the average phase speed, v_p) moving partons, the induced charge density is found to carry the oscillations along the direction of moving charge (as seen in Fig.3), which generate the Cerenkov like radiation and Mach shock waves. This oscillatory behaviour is always found, but the presence of magnetic field dampens the oscillation much. Because the real part of dielectric response function gets enhanced due to the presence of strong magnetic field (as illustrated in the right panel of Fig.1) and results a decrease in the amplitude.

On the other hand, for smaller parton velocities ($v = 0.55$), magnetic field does not alter the induced charge density significantly, because the real part of the dielectric function in the similar case (seen in the left panel of Fig.1) does not change much in the presence of magnetic field.

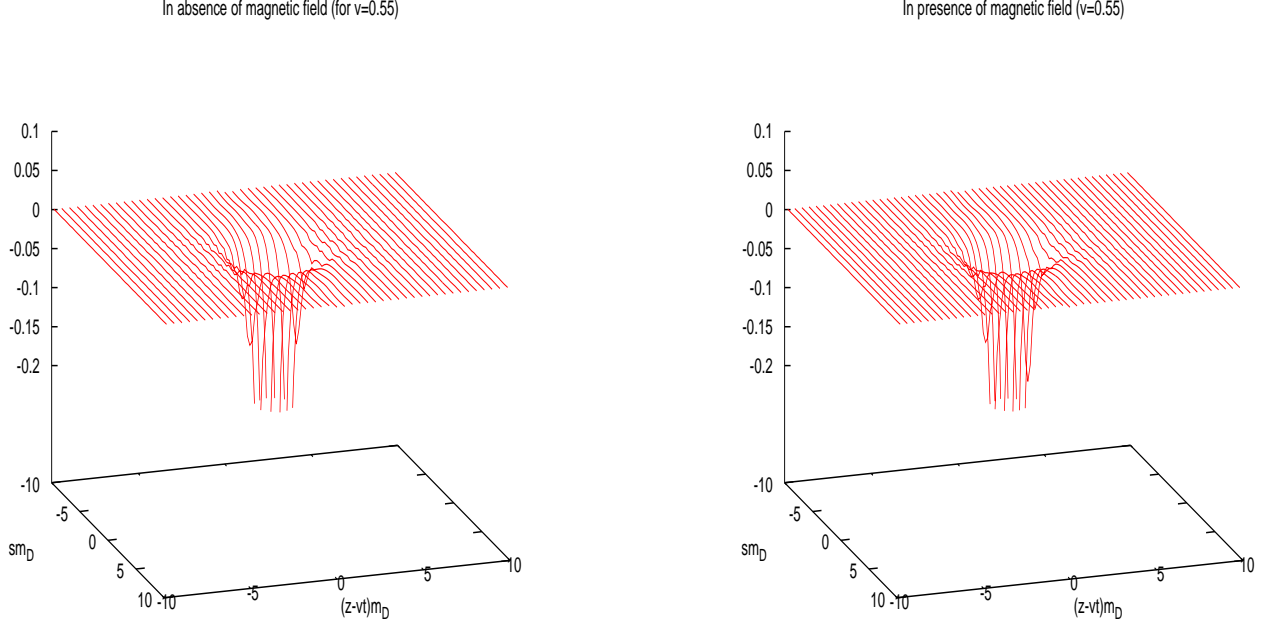


Figure 4: Scaled induced charge density (ρ_{ind}^0) in absence (Left panel) and presence (Right panel) of strong magnetic field for smaller parton velocity $v = 0.55$, respectively.

3.2 Wake potential

In this subsection we will study the wakes in the potential due to the induced charge density as discussed in the previous subsection. The wake potential in the momentum space is obtained from the Poisson equation as

$$\Phi^a(k_0, \mathbf{k}) = \frac{\rho_{\text{ext}}^a(k_0, \mathbf{k})}{k^2 \epsilon^{L'}(k_0, \mathbf{k})}. \quad (57)$$

Substituting the external color charge density from (53), the inverse Fourier transform gives the wake potential in the coordinate space

$$\Phi^a(\mathbf{r}, t) = Q^a \int \frac{d^3 k}{(2\pi)^3} \int e^{i(\mathbf{k} \cdot \mathbf{r} - \mathbf{k} \cdot \mathbf{v} t)} \frac{1}{k^2 \epsilon^{L'}(\mathbf{k} \cdot \mathbf{v}, \mathbf{k})}. \quad (58)$$

Similar to the coordinate transformations used for obtaining the induced charge density, we obtain the wake potential in the coordinate space

$$\Phi^a(\mathbf{r}, t) = \frac{Q^a}{2\pi^2} \int_0^\infty dk \int_0^1 d\chi J_0(ks\sqrt{1-\chi^2}) \left[\frac{\cos \Gamma \Re \epsilon^{L'}(kv\chi, \mathbf{k})}{\Delta} + \frac{\sin \Gamma \Im \epsilon^{L'}(kv\chi, \mathbf{k})}{\Delta} \right], \quad (59)$$

which will be computed for two directions, one is along the direction of motion of the partons ($\mathbf{r} \parallel \mathbf{v}$) and other is perpendicular to the direction of motion of the partons ($\mathbf{r} \perp \mathbf{v}$). Therefore,

the scaled wake potential along the direction of motion (we presumed that the partons are moving along the z-direction, i.e. $s = 0$) is thus obtained as

$$\Phi_{\parallel}^0(\mathbf{r}, t) = \int_0^{\infty} dk \int_0^1 d\chi \left[\frac{\cos \Gamma \Re \epsilon^{L'}(kv\chi, \mathbf{k})}{\Delta} + \frac{\sin \Gamma \Im \epsilon^{L'}(kv\chi, \mathbf{k})}{\Delta} \right], \quad (60)$$

and the potential perpendicular to the direction of motion is ($\Gamma' = k\chi vt$)

$$\Phi_{\perp}^0(\mathbf{r}, t) = \int_0^{\infty} dk \int_0^1 d\chi J_0(ks\sqrt{1-\chi^2}) \left[\frac{\cos \Gamma' \Re \epsilon^{L'}(kv\chi, \mathbf{k})}{\Delta} - \frac{\sin \Gamma' \Im \epsilon^{L'}(kv\chi, \mathbf{k})}{\Delta} \right]. \quad (61)$$

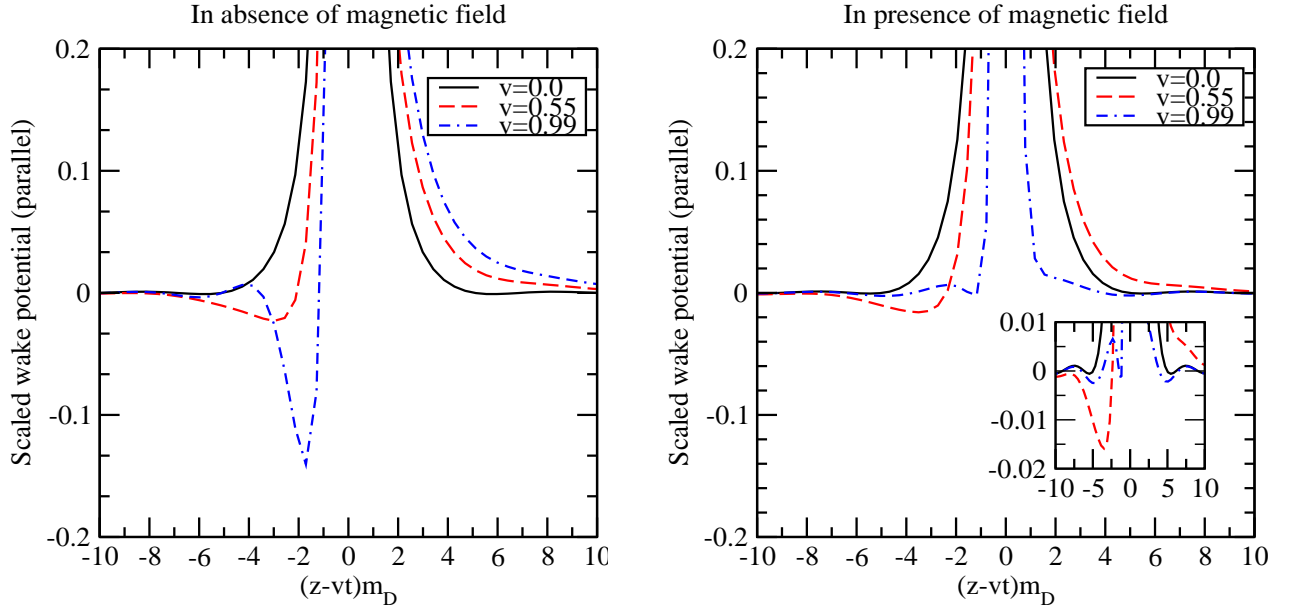


Figure 5: Left panel: Scaled wake potential (Φ_{\parallel}^0) along the motion of the partons for smaller and higher parton velocities in the absence of magnetic field. Right panel: Same as the left panel but in the presence of magnetic field.

Finally, to visualize the effects of magnetic field, we have computed the wake potential both in absence and presence of strong magnetic field along the parallel and perpendicular directions in Fig.5 and Fig.6, respectively. In the absence of magnetic field (left panel of Fig.5), for the static case, the wake potential is by default forward backward symmetric but for finite v it falls off very fast compared to the static one and loses the forward backward symmetry. In the backward region, the wake potential decreases with the distance and shows a minimum when partons move with

the velocity $v = 0.55$ (less than v_p). However for parton velocity greater than v_p , i.e. $v = 0.99$, the wake potential shows an oscillatory behavior and behaves differently from $v = 0.55$ case and the width of the negative minimum is increased and shifted towards the origin compared to $v = 0.55$. Thus in the backward region, the wake potential is a Lennard-Jones potential type which shows a short-range repulsive part and a long-range attractive part. On the other hand, in the forward region, the wake potential behaves more like a screened Coulomb potential and attains the Coulomb form on increasing the value of parton velocity. Thus the forward part is not much affected by the motion of charged particles. Now, in the presence of magnetic field (right panel of Fig.5), in the backward region the wake potential decreases on increasing the value of $(z - vt)m_D$, and shows a minimum but the depth of the minimum is in general decreased compared to the absence of magnetic field. For $v = 0.55$ the width has been reduced slightly, however for $v = 0.99$, the reduction is very large. Moreover, in the backward region for $v = 0.99$, the potential also shows oscillatory behavior but with lesser amplitude. This can be understood again in terms of enhancement of real part of dielectric response function in presence of magnetic field (seen in Fig.1). Thus in the backward region, the wake potential is still found to be of Lennard-Jones type potential. On the other hand in the forward region, the wake potential is screened Coulomb potential. However, for higher parton velocity, it does not attain the Coulomb form as found in the case when there is no magnetic field, rather it becomes more screened on increasing the value of parton velocity. Overall the magnetic field is found to affect the higher velocity partons only.

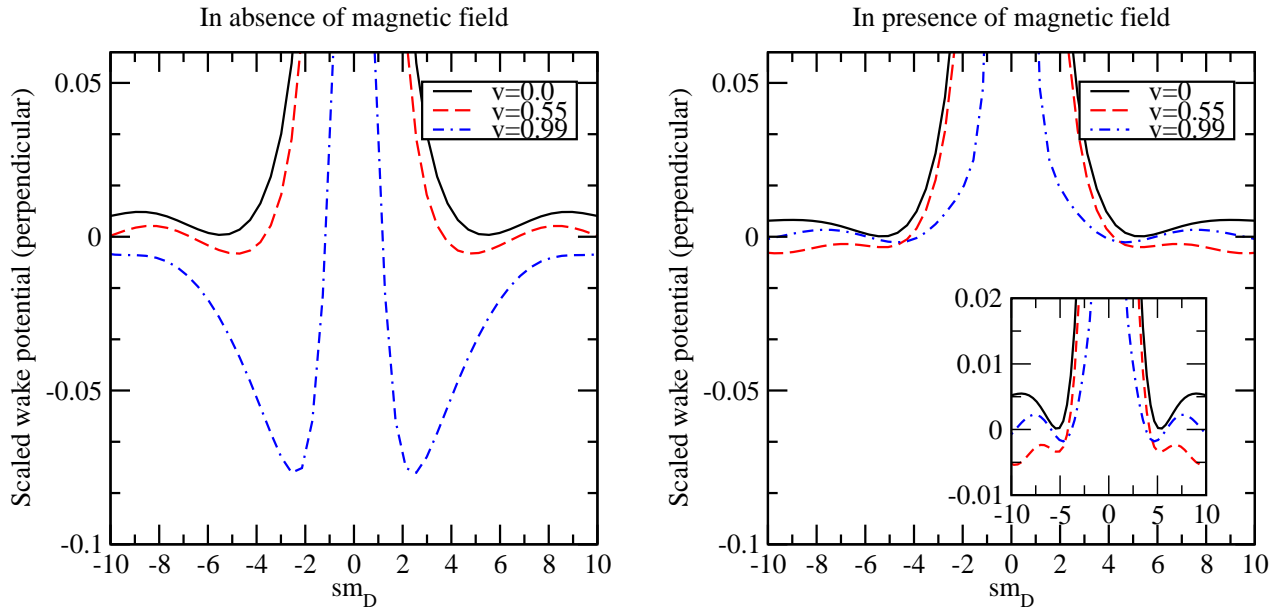


Figure 6: Left panel: Scaled wake potential (Φ_{\perp}^0) perpendicular to the direction of motion of the partons for smaller and higher parton velocities in the absence of magnetic field. Right panel: Same as the left panel but in the presence of magnetic field.

In absence of magnetic field, the wake potential, perpendicular to the moving partons (left panel of Fig.6), is symmetric in backward and forward regions, independent of the speed of the moving partons and the depth of negative minimum increases with the velocity of parton. The nature of wake potential is Lennard-Jones type for negative as well as positive value of sm_D . On the other hand, in the presence of strong magnetic field (right panel of Fig.6), the potential has the forward backward symmetry and of Lennard-Jones nature. However, the magnetic field decreases the depth of negative minimum for higher parton velocity, which is opposite to the absence of magnetic field.

4 Conclusions

In the present study we have calculated the wakes in the induced charge density as well as in the potential generated due to the passage of highly energetic partons through a thermal QCD medium in the presence of strong magnetic field, believed to be created in the off central events of heavy-ion collision experiments. For that purpose we have calculated the responses of the medium both in presence and absence of strong magnetic field through the dielectric function. To calculate the response function, first we have revisited the general covariant form for the one-loop gluon self-energy tensor at finite temperature and finite magnetic field and then approximated the relevant structure functions at finite temperature in the strong magnetic field limit. Thus we have obtained the real and imaginary parts of complex dielectric response function both in absence and presence of strong magnetic field for slow ($v = 0.55$) and fast ($v = 0.99$) moving partons. For slow moving partons, we have found that the real part of dielectric response function is not much

affected by the magnetic field whereas for fast moving partons, it becomes very large compared to its counterpart in absence of magnetic field for small $|\mathbf{k}|$, however, it approaches towards the value in absence of magnetic field for large $|\mathbf{k}|$. On the other hand the magnitude of the imaginary part of dielectric response function is slightly decreased for both slow and fast moving partons in presence of strong magnetic field. Finally, we have computed the scaled induced charge density (ρ_{ind}^0) and the scaled wake potential for parallel (Φ_{\parallel}^0) and perpendicular (Φ_{\perp}^0) directions to the motion of moving partons. The oscillation found in ρ_{ind}^0 due to the very fast partons becomes less pronounced in the presence of strong magnetic field whereas for smaller parton velocity, no significant change is observed. The wake potential, Φ_{\parallel}^0 for very fast moving partons is found to be of Lennard-Jones (LJ) type and the depth of negative minimum in the backward region is reduced drastically, resulting in the decrease of amplitude of oscillation due to the strong magnetic field. On the other hand in the forward region, Φ_{\parallel}^0 remains the screened Coulomb one, except the screening now becomes relatively stronger for higher parton velocity. For Φ_{\perp}^0 in both forward and backward region, the depth of negative minimum in LJ potential gets decreased severely for fast moving partons, but still retains the forward-backward symmetry. However, for lower parton velocity, the magnetic field does not affect the nature of Φ_{\perp}^0 significantly.

Acknowledgements

BKP is thankful to the CSIR (Grant No.03 (1407)/17/EMR-II), Government of India for the financial assistance.

References

- [1] R. Baier, Y. L. Dokshitzer, A. H. Mueller and D. Schiff , Phys. Rev. D **58**, 1706 (1998).
- [2] B. G. Zakharov, JETP Lett. **65**, 615 (1997).
- [3] R. Baier, Y. L. Dokshitzer, A. H. Mueller and D. Schiff, JHEP **0109**,033 (2001).
- [4] A. Kovner and U. A. Wiedermann, hep-ph/0304151.
- [5] M. Gyulassy and X. Wang, Nucl. Phys. **420**, 583 (1994).
- [6] M. Gyulassy, P. Levai, and I. Vitev, Nucl. Phys. B **594**, 371 (2001).
- [7] M. G. Mustafa and M. H. Thoma, Acta Physica Hungarica A **22**, 93 (2005).
- [8] M. G. Mustafa, Phys. Rev. C **72**, 014905 (2005).
- [9] S. Wicks, W. Horowitz, M. Djordjevi and M. Gyulassy, Nucl. Phys. A **783**, 493 (2007).
- [10] G.-Y. Qin, J. Ruppert, C. Gale, S. Jeon, G. D. Moore and M. G. Mustafa, Phys. Rev. Lett. **100**, 072301 (2008).

- [11] B. G. Zakharov, JETP Lett. **88**, 781 (2008).
- [12] M. Gyulassy and M. Plümer, Phys. Lett. B **243**, 432 (1990).
- [13] E. Wang and X.-N. Wang, Phys. Rev. Lett. **89**, 162301 (2002).
- [14] J. D. Bjorken, Report No. Fermilab-Pub-82/59-THY, 1982.
- [15] J. Adams et al. (STAR Collaboration), Phys. Rev. Lett. **95**, 152301 (2005).
- [16] S. S. Adler et al. (PHENIX Collaboration), Phys. Rev. Lett. **97**, 052301 (2006).
- [17] V. Greco, C.M. Ko and P. Levai, Phys. Rev. Lett. **90**, 202302 (2003).
- [18] R. C. Hwa and C.B. Yang, Phys. Rev. C **70**, 024905 (2004).
- [19] J. Casalderrey-Solana, E. V. Shuryak and D. Teaney, J. Phys. Conf. Ser. **27**, 22 (2005).
- [20] J. Casalderrey-Solana, J. Phys. G **34**, S345 (2007).
- [21] H. Stoecker, Nucl. Phys. A **750**, 121 (2005).
- [22] V. Koch, A. Majumder and Xin-Nian Wang, Phys. Rev. Lett. **96**, 172302 (2006).
- [23] A. Majumder and Xin-Nian Wang, Phys. Rev. C **73**, 051901 (2006).
- [24] J. Ruppert and B. Müller, Phys. Lett. B **618**, 123 (2005).
- [25] J. Ruppert, Nucl. Phys. A **774**, 397 (2006).
- [26] P. Chakraborty, M. G. Mustafa, and M. H. Thoma, Phys. Rev. D **74**, 094002 (2006).
- [27] B.-f. Jiang and J.-r. Li, Nucl. Phys. A **832**, 100 (2010).
- [28] P. Chakraborty, M. G. Mustafa, R. Ray, and M. H. Thoma, J. Phys. G **34**, 2141 (2007).
- [29] M. Mandal and P. Roy, Phys. Rev. D **86**, 114002 (2012).
- [30] M. Mandal and P. Roy, Phys. Rev. D **88**, 074013 (2013).
- [31] B.-f. Jiang and J.-r. Li, Nucl. Phys. A **856**, 121 (2011).
- [32] L. Liu and H. Liu, Phys. Rev. D **93**, 085011 (2016).
- [33] V. Skokov, A. Illarionov, V. Toneev, Int. J. Mod. Phys. A **24**, 5925 (2009).
- [34] V. Voronyuk, V. D. Toneev, W. Cassing, E. L. Bratkovskaya, V. P. Konchakovski, S. A. Voloshin, Phys. Rev. C **83**, 054911 (2011).
- [35] K. Tuchin, Adv. High Energy Phys. 2013, 490495 (2013),
- [36] L. McLerran, V. Skokov, Nucl. Phys. A **929**, 184 (2014).
- [37] S. Rath and B. K. Patra, Phys. Rev. D **100**, 016009 (2019).

- [38] Kenji Fukushima, Dmitri E. Kharzeev and Harmen J. Warringa, Phys. Rev. D **78**, 074033 (2008).
- [39] V. Braguta, M. N. Chernodub, V. A. Goy, K. Landsteiner, A. V. Molochkov and M. I. Polikarpov, Phys. Rev. D **89**, 074510 (2014).
- [40] Dmitri E. Kharzeev and Dam T. Son, Phys. Rev. Lett. **106**, 062301 (2011).
- [41] V. P. Gusynin, V. A. Miransky and I. A. Shovkovy, Phys. Rev. Lett. **73**, 3499 (1994).
- [42] A. Weldon, Phys. Rev. D. **26**, 1394 (1982).
- [43] J. I. Kapusta, Finite Temperature Field Theory, Cambridge University Press, Cambridge, 1989.
- [44] M. LeBellac, Thermal Field Theory, Cambridge University Press, Cambridge, 2000.
- [45] E. Braaten and R. D. Pisarski, Phys. Rev. Lett. **64**, 1338 (1990).
- [46] R. Kobes, G. Kunstatter and K. Mak, Phys. Rev. D **45**, 4632 (1992).
- [47] K. Hattori and D. Satow, Phys. Rev. D **97**, 014023 (2018).
- [48] K. Hattori and K. Itakura, Ann. Phys. (N.Y.) **330**, 23 (2013).
- [49] R. L. Kobes, G. W. Semenoff, Nucl. Phys. B **260**, 714 (1985).
- [50] E. J. Ferrer, V. de la Incera, and X. J. Wen, Phys. Rev. D **91**, 054006 (2015).
- [51] V. P. Gusynin, V. A. Miransky, and I. A. Shovkovy, Nucl. Phys. B **462**, 249 (1996).
- [52] K. Fukushima, Phys. Rev. D **83**, 111501(R) (2011).
- [53] K. Hattori and K. Itakura, Ann. Phys. (N.Y.) **334**, 58 (2013).
- [54] M. Hasan, B. Chatterjee and B. K. Patra, Eur. Phys. J. C **77**, 767 (2017).
- [55] S. Mandelstam, Phys. Rev. D **11**, 3026 (1975).
- [56] A. V. Smilga, Phys. Lett. B **278**, 371 (1992).
- [57] K. Fukushima, J. Phys. G **39**, 013101 (2012).
- [58] K. Fukushima, K. Hattori, Ho-Ung Yee and Yi Yin, Phys. Rev. D **93**, 074028 (2016).
- [59] A. Bandyopadhyay, C. A. Islam and M. G. Mustafa Phys. Rev. D **94**, 114034 (2016).
- [60] E. Braaten and R. D. Pisarski, Nucl. Phys. B **337**, 569 (1990).
- [61] R. D. Pisarski, Phys. Rev. Lett. **63**, 1129 (1989).
- [62] M. H. Thoma, arXiv:[hep-ph]/0010164.
- [63] Mikko Laine and York Schröder, JHEP 03 (2005).